ANZIAM J. 59(2017), 35–50
doi:10.1017/S1446181117000281

TRUCK SAFETY BARRIERS FOR MINING SITES

NEVILLE FOWKES[1], STEVE DURKIN[2] and ANDREW P. BASSOM[✉3]

(Received 12 February, 2017; accepted 19 May, 2017; first published online 31 July 2017)

Abstract

Safescape is a Western Australian company that has recently developed a device for improved safety in open-pit mines. Serious accidents can occur when large trucks veer off the roads running around the edge of the mine. The conventional technique to mitigate the risk is to pile waste rock to form a so-called bund on the edge of the road. This method is not fail safe though as vehicles can, and do, drive completely over the bund. In this paper, we describe a new device that consists of a row of filled polyethylene shell units which are linked together and sit on the road side of the rock bund. The vertical front face of the edge protector prevents out of control dump trucks from climbing over the bund and into the pit, so that they push against the barriers and heave the broken rock behind the bund. The models developed here suggest that the primary resistance to an impacting truck is provided by the large heaving force with the barrier simply facilitating this process. The theory indicates that the total resistance is independent of truck speed, meaning that simple barrier pushing experiments are sufficient to validate the analysis. The conclusions of the theory and field tests suggest that in a worst-case scenario involving the normal impact of a 500 tonne filled dump truck, the barriers and bund move a few metres before coming to rest.

2010 *Mathematics subject classification*: primary 74C15; secondary 74M20.

Keywords and phrases: mining safety, impact, soil mechanics.

1. Introduction

Modern open-pit mines are typically enormous structures; for instance, mines are often a few kilometres long and wide and over half a kilometre deep. Large trucks are used to move soil and rock around the sites and these vehicles can be as heavy as 500 tonnes when fully loaded. Cut into the side of the mines are the haul roads on which the trucks travel, and a real danger is that if trucks leave the haul roads, they fall into the pit below with catastrophic consequences for both the equipment and the personnel.

[1]School of Mathematics and Statistics, University of Western Australia, Crawley, WA 6009, Australia; e-mail: neville.fowkes@uwa.edu.au.
[2]Safescape, Forrestfield, WA 6056, Australia; e-mail: steve@safescape.net.au.
[3]School of Physical Sciences, University of Tasmania, Private Bag 37, Hobart, TAS 7001, Australia; e-mail: andrew.bassom@utas.edu.au.

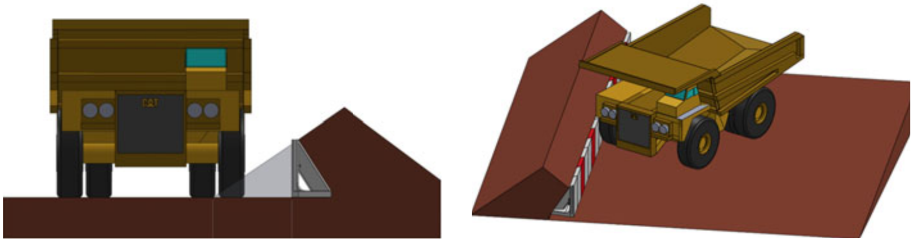

FIGURE 1. A schematic of the EP system. The barrier sits on the road side of the bund with a vertical face showing to any vehicle that impacts with the bund.

This eventuality occurs more often than might be expected; drivers tend to work long hours under boring conditions, so are prone to lose concentration. In order to minimize the chance of serious accidents, the usual approach taken is to pile a quantity of loose rock (called a bund) on the edge of the haul road so that if a truck leaves the road, it strikes the bund and either deflects off or partially climbs over it and is brought to rest.

Unfortunately, this measure is not sufficient to eliminate accidents altogether. Trucks travel at relatively high speeds, and incidents have been documented when out of control vehicles have travelled right over the top of the bund into the pit below. Haul roads are expensive to build, and efficient mining requires that they are no wider than absolutely essential. One obvious way to eliminate the possibility of trucks completely passing over the bund would be to build a huge pile of rock on the side of the road, but the cost of constructing such a large mound is prohibitive and would significantly reduce the area being mined over the whole site.

In an effort to address this problem, a West Australian company (Safescape) has been developing a new device, known as an edge protector (EP) barrier, which is designed to create a vertical front face to a conventional broken rock safety bund. A sketch of the configuration of the barrier is shown in Figure 1. The fundamental premise of the product is that by creating a vertical front face to the bund, trucks cannot roll up and over the bund and, instead, have to push against (and through) the barrier. Only if the truck struck the barrier with sufficient force to push both the obstacle and all the bund behind it into the pit, would the vehicle be in real danger itself. The barrier is not attached to the ground and under impact will move, and this will heave the crushed rock bund behind it. The resulting resistance is large and will ideally either bring the dump truck to rest or deflect it back onto the road. The resistance to movement will be a function of both the barrier dimensions and the bund size, and ideally the barrier should fulfil twin but conflicting aims. On the one hand, the barrier needs to be sufficiently yielding that the damage to life and the truck is minimized, but at the same time robust enough to prevent the truck passing through the bund and over the pit edge.

The edge protectors are polyethylene shells which are filled with polyurethane, although on-site sand-fill or paste-fill material could be used as a convenient alternative. The vertical face of the structures are roughly square with edge of about

FIGURE 2. The EP prototype units. The main features are evident: a square vertical face with a horizontal base and a support strut. On site the shell is filled with a suitable material.

FIGURE 3. A loader placing rock material behind the units at the Edna May mine in Western Australia. The separate panels are linked together to form a vertical face behind which the top of the bund can be seen. Approximate dimensions can be estimated relative to the worker in the foreground.

2 m; the units also have a horizontal base and support is provided by a strut (see Figure 2). These panels are loosely linked together and are aligned so as to skirt the haul road as shown in Figure 3. The rock fill is loosely packed against the back of the barrier, and the loading of rock on the base of the panel keeps the barrier vertical under both resting and impact conditions. The barrier is not anchored to the ground and is free to slide under impact. The units are designed to be sufficiently structurally strong both to support the broken rock bund and to keep the face vertical if shunted by a truck. It is anticipated that under realistic impact conditions, the device will not escape unscathed and is likely to suffer some, hopefully only superficial, damage.

https://doi.org/10.1017/S1446181117000281 Published online by Cambridge University Press

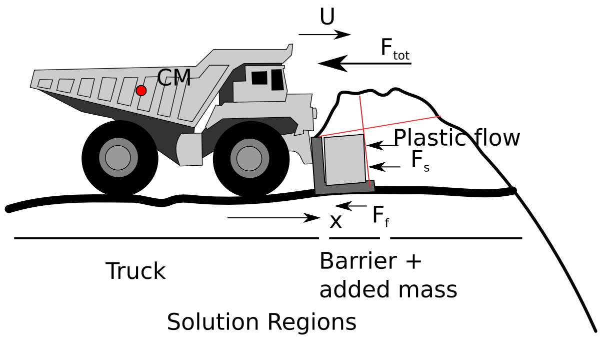

FIGURE 4. Schematic of the normal incidence of a truck and the barrier. The total force F_{tot} acting to reduce the speed is composed of the friction on the barrier base F_f and the force due to the moving soil F_s. Notice in particular that the height of the bund is typically greater than that of the barrier.

The work described in this paper arose from the need to understand some of the key factors that underpin the design of the units. While many of the early field tests were largely empirical in nature, it was felt that a theoretical appreciation of relevant models would be valuable. We examine the problem more deeply in the work described below, and start in Section 2 with a consideration of a simple interaction between the truck, the barrier and the bund. Here we are concerned with what seems to be the worst-case scenario in which the truck impacts the barrier head-on, and some crude estimates of the barrier resistance forces and the depth of penetration of the barrier can be made. Such estimates may be used to gauge the effect of the impact on both the driver and the truck itself. Given these initial results, we next examine in Section 3 a more detailed description of the movement of the bund behind the barrier and the associated heaving force. Our predictions are benchmarked against the results of some on-site experiments that are described in Section 4. The paper concludes with some final remarks in Section 5.

2. A first model of an impact between a truck and the barrier

We start by considering a very simplified model of the interaction when a truck impacts the barrier at right angles to the line of units. In simplest terms we can think of the decelerating force acting on the truck as arising in two ways: there is the friction on the base of the barrier as it is forced to move, and there is the resistance arising from the movement of the soil or rock in the bund. The plastic flow of the soil requires more detailed modelling, which is postponed to Section 3. For the moment, we just assume that the force provided by the soil is given. A schematic of the situation is sketched in Figure 4, which illustrates the approximate relative sizes of the components of the system. If the truck impacts the barrier at a speed U, then at a later time t we shall suppose that the truck has moved a distance $x(t)$ and is subject to a total resistive force of F_{tot} comprising the friction component F_f and the soil component F_s.

If we make the reasonable assumption that as soon as the truck strikes the barrier the driver takes his foot off the accelerator, the equation of motion of the rolling truck is simply

$$M\frac{d^2x}{dt^2} = -F_{\rm tot}, \quad \text{subject to } x(0) = 0 \quad \text{and} \quad \frac{dx}{dt}(0) = U,$$

where M is the mass of the truck. Our ultimate aim is to determine $F_{\rm tot}$ as a function of the barrier dimensions and weight, the soil pile size, density and shear strength and the velocity and size of the dump truck with or without load.

Of particular interest is the penetration distance x_p that the system moves before motion ceases. To estimate x_p, it is helpful to formulate the problem in terms of energy loss. The truck loses energy by pushing against the barrier and soil pile, and if the work done is sufficient to bring the truck to rest then

$$\int_0^{x_p} F_{\rm tot}\, dx = \frac{1}{2}MU^2.$$

In general, one might expect $F_{\rm tot}$ to be a function of the speed of the barrier but should $F_{\rm tot}$ be constant, this gives a penetration distance

$$x_p = \frac{MU^2}{2F_{\rm tot}}. \tag{2.1}$$

The frictional component F_f of the total friction force is given by

$$F_f = \mu(m_b + m_a)g, \tag{2.2}$$

where μ is the effective frictional coefficient between the ground and the barrier, and m_b and m_a denote the barrier mass and added mass of soil contained by the barrier, respectively.

The soil resistance component F_s is rather harder to access, but we do know that the soil will move locally if the maximum shear strength $S_{\max}$ is exceeded, and classical elasticity theory tells us that its value at a point in an elastic solid is the average of the maximum and minimum principal stresses (σ_1, σ_3). Thus, $S_{\max} = (\sigma_1 + \sigma_3)/2$ and, furthermore, its direction should make an angle $\pi/4$ with each of the two principal directions. In our context, one would expect that the maximum principal stress σ_3 is aligned with the truck movement, and

$$\sigma_3 = 2S_{\max} - \sigma_1.$$

In the vertical direction the pressure is hydrostatic, so that the average minimum principal stress is given by $\sigma_1 = -\rho_s gh/2$, where h is the height of the barrier and ρ_s the density of the soil. Thus, the total soil force F_s acting against the truck is given by

$$F_s = hl(2S_{\max} + \tfrac{1}{2}\rho_s gh), \tag{2.3}$$

where l is the width of the barrier. Given the expressions (2.2) and (2.3) for the two friction components, it is helpful to be able to assess their approximate values. Of

https://doi.org/10.1017/S1446181117000281 Published online by Cambridge University Press

course this relies on some experimental estimates. For a typical barrier size of height 2 m and a footing of 1 m, the mass of the barrier m_b is roughly 5600 kg and the added mass due to the bund sitting on the footing is, perhaps, 12 800 kg. It is thought that the effective coefficient of friction between the barrier and the ground is about 0.4 and taken together the frictional drag force F_f is about 270 kN. Turning to the soil friction, the text by Capper and Cassie [1] suggests that the maximum shear strength $S_{\max}$ might lie anywhere between about 30 and 300 kN m^{-2}, depending on whether the soil is sand or clay. The density ρ_s of the soil is likely to be anywhere between about 1200 and 2800 kg m^{-3}, depending on whether the bund is fairly loose or compacted after ramming. Either way, this suggests that the soil friction is typically between about 380 and 520 kN m^{-2}, and is likely to be significantly larger than the frictional component. Furthermore, based on these values, the prediction (2.1) suggests that an empty truck which impacts the barrier at 20 km hr^{-1} might penetrate the bund to a distance of about 9 m, while a full truck travelling more slowly at 15 km hr^{-1} would be brought to rest in about two-thirds of that distance. In our simple analysis, the stopping distance increases with the square of the initial velocity, and is inversely proportional to the reaction force, which is dominated by the soil component. This part grows with barrier dimensions, and is sensitive to both the soil type and density. The primary purpose of the barrier is thus to enable the force transmitted by the impacting truck to be transferred to the soil behind the barrier, which dissipates the kinetic energy.

Whilst this simple model extracts some of the major features of the problem, there are important questions that have been circumvented. Among these, a key issue from a practical point of view is the effect the bund geometry plays in determining the soil resistance force. Is it the height of the barrier, or is it the size of the bund that is the more significant? A related issue is how the rock particles might be heaved up and over the barrier as the obstacle moves into the bund, and how this might be accounted for in the model. Unfortunately, neither of these issues can be resolved immediately, and require a detailed analysis of the soil movement behind the barrier.

3. An analysis of soil heave

The pure plasticity model as described in the classic book by Hill [5] was the first theory forwarded as a practical way to describe the shear yielding of metals under external forcing. A soil also yields in shear under external forcing, but there are significant differences in behaviour, which means that the plasticity model is not immediately applicable, although in both instances a yield criterion can be derived whose satisfaction implies that plastic flow will ensue. The criterion takes the generic form $f(J_1, J_2, J_3) = 0$, where $J_i(\sigma_1, \sigma_2, \sigma_3)$ are the stress invariants and σ_i are the principal stress components.

Over the years two models have gained general acceptance for describing the yielding of metal.

- The Tresca yield condition is the more frequently used and states that yield occurs if the maximum shear stress $S_{\max}$ exceeds the yield value. In the soil

https://doi.org/10.1017/S1446181117000281 Published online by Cambridge University Press

case, the equivalent result is the so-called Mohr–Coulomb model

$$S_{\max} = c - \sigma \tan\phi,$$

where c denotes the apparent cohesion coefficient, σ is the normal component of stress and ϕ is the internal resistance angle (see the book by Capper and Cassie [1]). We remark that the two constants specify the soil behaviour under yielding conditions, and these need to be determined using a triaxial test. However, if the loading occurs rapidly, as is the case in our truck example, the cohesion term is the dominant one.

- An alternative to the Tresca description is provided by the von Mises condition

$$(\sigma_1')^2 + (\sigma_2')^2 + (\sigma_3')^2 = 2k^2,$$

which is generally easier to apply. Here $\sigma_i' = (\sigma_i - p)$ (where p is the pressure) are reduced (deviatoric) principal stresses, and the result states that hydrostatic pressure does not cause yielding for metals, but rather that this occurs when the recoverable elastic energy reaches some critical value k. In the case of metals, k is determined by the stress history, but no such simple equivalent theory exists for soils. If the history of the soil is known, the degree of soil complication can be inferred and k then found.

The behaviour of a soil under stress is greatly dependent on its type, its degree of compaction and the degree of water saturation. Inorganic soils are generally divided into coarse-grained types which are noncohesive soils like gravels and sands, and fine-grained forms that are cohesive like silts and clays. Noncohesive soils resist movement frictionally, whereas cohesive soils act more plastically and are more like metals in this regard. The shear strength of a particular soil is affected by many factors including its composition, state, structure and loading conditions. Under the action of a shear force, a compact soil may first expand with shear stress levels reaching peak value and then reducing, as the soil softens until an equilibrium state is achieved. Beyond this point, the volume remains fixed and the stress/strain curve levels off. For a loose soil, the volume reduces and stress levels monotonically increase until this critical state is reached. Further complication arises should the soil be saturated, but then the behaviour depends on whether drainage can occur over the time scales of interest. Usually when stress is applied suddenly, there is insufficient time for water to drain from the soil and the volume of soil is unaltered. In our truck problem we expect there to be a short initial transient interval followed by a constant-volume stage irrespective of whether the soil is wet; a constant-volume critical-state model is therefore appropriate. Then it can be shown that the effective angle of shearing resistance is almost zero, so that the Tresca model can be used (see the book by Capper and Cassie [1] or the article by Chan [2]). In our on-site situation, there are rocks of various sizes and clay, but one would expect the movement to be controlled by the lubricating clay.

In passing, we note that a dynamical systems model of shear flow has been developed more recently by Joseph [6]. Whilst this formulation is mathematically and conceptually elegant, there seems to be no significant practical advantage in adopting this more complicated approach for our application. Nevertheless, the reader seeking a more contemporary account of plasticity theory and its mathematical foundation is directed to either [3] or [7].

3.1. Perfect plasticity theory under plane flow conditions There are very few exact solutions for perfect plastic flow but for our problem with a two-dimensional steady state configuration such a solution can be identified. One feature of this model is that there is no elastic zone that separates the rigid body and plastic zones. This has the advantage that it greatly simplifies the model description but unfortunately creates some technical difficulties; one is forced to accept that discontinuities in the tangential components of velocities and stresses can occur across slip-lines. A more complete theory would be much more complicated and thus theoretically more satisfactory but not practically useful.

Consider a flow in the (x, y) plane with velocity components (u_x, v_y) in these directions. This is the movement induced behind the barrier and, since there is no shear out of the (x, y) plane, the components $\tau_{xz} = \tau_{yz} = 0$, which in turn implies that σ_z is a principal stress. Since we assume that there is no volume change, the stress state is one of pure shear τ and hydrostatic pressure p, which means that $\sigma_z = -p$, $(\sigma_x, \sigma_y) = -p \pm \tau$ and

$$\sigma_z = \tfrac{1}{2}(\sigma_x + \sigma_y) \equiv \tfrac{1}{3}(\sigma_x + \sigma_y + \sigma_z).$$

Equilibrium requires that

$$\frac{\partial \sigma_x}{\partial x} + \frac{\partial \tau_{xy}}{\partial y} = 0, \tag{3.1a}$$

$$\frac{\partial \tau_{xy}}{\partial x} + \frac{\partial \sigma_y}{\partial y} = 0 \tag{3.1b}$$

and a constant volume is ensured if

$$\frac{\partial u_x}{\partial x} + \frac{\partial v_y}{\partial y} = 0. \tag{3.2}$$

The slope of the principal axis of stress with respect to the x-axis θ is given by

$$\tan 2\theta = \frac{2\tau_{xy}}{\sigma_x - \sigma_y},$$

whilst the slope θ' of the principal axis of strain rate is given by

$$\tan 2\theta' = \frac{(u_x)_y + (v_y)_x}{(u_x)_x - (v_y)_y},$$

where a subscript exterior to quantities of the form $(\cdot)$ denotes a partial derivative. For these to coincide,

$$\frac{2\tau_{xy}}{\sigma_x - \sigma_y} = \frac{(u_x)_y + (v_y)_x}{(u_x)_x - (v_y)_y}. \tag{3.3}$$

We point out that the bund will be isotropic on a sufficiently large length scale and that for an isotropic plastic material the principal axes of stress and strain rate must coincide, as noted by Hill [5].

https://doi.org/10.1017/S1446181117000281 Published online by Cambridge University Press

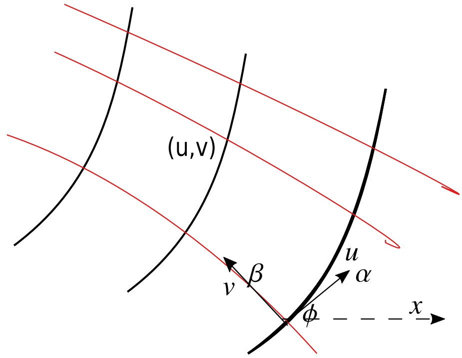

FIGURE 5. A sketch of the slip-line geometry. Shown are the two families of slip-lines with α or β constant. The velocity components are taken to be (u, v) along the α,β slip-lines, respectively. The angle ϕ is measured in an anticlockwise direction from the x-axis to the α slip-line.

The yield condition determines when slip occurs; we can use either the von Mises or the Tresca model, as both are described by

$$\tau^2 = \tfrac{1}{4}(\sigma_x - \sigma_y)^2 + \tau_{xy}^2 = k^2. \tag{3.4}$$

Note that in the Tresca formulation $k = Y/2$, while in the von Mises scenario $k = Y/\sqrt{3}$, where Y denotes the yield stress in uniaxial tension with $\sigma_1 = Y$ and $\sigma_2 = \sigma_3 = 0$.

We now have the five equations (3.1a), (3.1b), (3.2)–(3.4) to be solved for the five unknowns $\sigma_x, \sigma_y, \tau_{xy}, u_x$ and v_y. Notice in particular that the time t does not appear explicitly in the equations, so stresses are independent of the rate of strain.

3.2. Slip-lines The technique required to solve the hyperbolic plastic flow problem (analytically or numerically) is based on the method of characteristics, which are referred to as slip-lines in the plastic flow context. There are two distinct orthogonal characteristic directions α and β, which one identifies with the maximum shear-strain directions. The state of stress throughout the domain is completely known, given the orientation ϕ of the α slip-line relative to the x-axis and the mean normal stress $-p$ throughout the domain; explicitly,

$$\sigma_x = -p - k\sin 2\phi, \quad \sigma_y = -p + k\sin 2\phi \quad \text{and} \quad \tau_{xy} = k\cos 2\phi.$$

We see then that the determination of the slip-lines is the central issue. Their positioning is dependent on the solution itself, so that isolating their locations is often not a trivial matter. It is helpful to consider the problem relative to the α and β lines as shown in Figure 5 and suppose that the velocity components along these lines are u and v, respectively. Along the slip-lines, the defining plastic flow equations reduce to very simple forms relating the variables (p, u, v, ϕ), where ϕ is the angle that an α slip-line makes with the x-axis. Along an α-increasing slip-line

$$du - v\,d\phi = 0, \tag{3.5}$$

https://doi.org/10.1017/S1446181117000281 Published online by Cambridge University Press

while on a β-increasing slip-line

$$dv + u\,d\phi = 0. \tag{3.6}$$

These results are simply mass conservation results and are equivalent to the continuity equation (3.2). Of course we can express the slip-line velocity components (u, v) in terms of the velocities (u_x, v_y) in the Cartesian directions. From elementary geometry,

$$u_x = u\cos\phi - v\sin\phi \quad \text{and} \quad v_y = u\sin\phi + v\cos\phi$$

or equivalently

$$u = u_x\cos\phi + v_y\sin\phi, \tag{3.7a}$$

$$v = v_y\cos\phi - u_x\sin\phi. \tag{3.7b}$$

Appropriate pressure conditions must also hold along the slip-lines. Along α and β slip-lines

$$p + 2k\phi = \text{const.}, \tag{3.8a}$$

$$p - 2k\phi = \text{const.}, \tag{3.8b}$$

respectively. It is now a matter of determining the slip-line geometry and associated variables, so that the above results fit together and are consistent with the imposed boundary conditions. The critical feature of the solution is that discontinuities in the tangential components of shear and velocity can only occur across the characteristics; the normal components need to be continuous. Somewhat surprisingly these requirements together are enough to uniquely determine the solution.

3.3. Construction of the solution for the dump truck problem Before we consider in detail the slip-line geometry for our present problem, it is worthwhile pausing to consider what we might expect to be the case. First, if the barrier with soil pile backing is too insubstantial then the dump truck will simply move the whole structure forwards, which is not desirable. The total pile therefore needs to be large enough so that yielding occurs within the pile and this will normally first occur near the top of the barrier. Over a relatively short time, there will be a rearrangement of rock particles, until the bund is hydrostatically supported with the barrier providing the required containment force; after that a quasi-steady situation arises. We remark that it is simplest to consider the situation relative to the coordinate frame that moves with the barrier at speed U. Then, in this frame, soil moves with speed $-U$ from the right onto the stationary barrier, as sketched in Figure 6. The triangular wedge of soil OSC remains rigid and attached to the barrier, and is separated from the soil moving with a steady speed $-U$ into the barrier by a plastic flow region indicated by the sector OCD in Figure 6.

The slip-line geometry consists of radial β slip-lines centred on the barrier top O with circular arcs as α slip-lines as shown. To see that this configuration fulfils the requirements of the problem, it is helpful to make the following observations. The

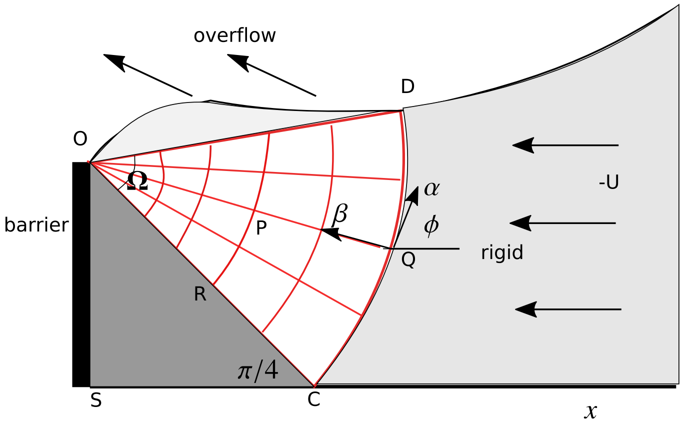

FIGURE 6. A sketch of the slip-line geometry within the frame which holds the barrier fixed. Slip occurs along the radial β slip-lines depicted (the red lines). The dynamic pressure increases in the azimuthal α direction away from the rigid body/plastic zone junction along slip-line OC. Soil in the wedge OSC is at rest; that to the right of the arc CQD moves with velocity $-U$ to the left. Soil overflows and spills above the barrier as shown; the net flux into the plastic region over CQD is balanced by the net overflow flux across OD.

maximum principal stress in the rigid region OSC will be in the x-direction, so that theory indicates that the direction of maximum shear will be inclined at $\pi/4$ to this direction and so is along the line OC. Slip therefore first occurs on this line which separates the "dead" rigid body region OSC from the plastic flow region OCD. Since the β slip-line OC is straight, an immediate consequence of the classical Hencky's theorem (see the book by Hill [5] for details) is that all the β slip-lines are likewise straight. Further appeal to this theorem tells us that the α slip-lines must be orthogonal to the radial β lines, so take the form of circular arcs with centre O.

We can now tackle the problem of determining the associated velocity field. The normal velocity u across the separating slip-line OC must be continuous and, since clearly $u = 0$ in the rigid region, it must also vanish along OC in the adjacent plastic flow region. Furthermore, the normal velocity u must be constant along any of the rays emanating from O, although this constant will vary from ray to ray and so is a function of angle ϕ. There is no equivalent statement that can be made about the tangential velocity along the slip-line OC (that is v), which is certainly not constant along the radial rays. On the other hand, this velocity component does need to be continuous across the separation slip-line CD, marking the boundary between the moving soil and the region of plastic flow. This requires that just inside CD in the plastic zone, the velocity v along the β streamlines must match that of the rigid moving zone, so that $v = U\sin\phi$ according to (3.7b).

With this knowledge, it is now possible to find the flow velocity $(u(\mathrm{P}), v(\mathrm{P}))$ at an arbitrary point P within the plastic flow region OCD of Figure 6. Along the radial line OQ, the angle ϕ is constant so that $d\phi = 0$ and $dv = 0$ according to (3.6). Thus, the

https://doi.org/10.1017/S1446181117000281 Published online by Cambridge University Press

velocity along each of the radial slip-lines remains constant, and so is the value taken at the boundary CD. Moreover, the results (3.8a) and (3.8b) imply that the pressure also remains constant along the radial slip-lines since $d\phi = 0$, so that

$$v = U \sin\phi \quad \text{and} \quad p = p(\phi). \tag{3.9}$$

Next consider the α slip-line RP. According to (3.5), we have $du = v\,d\phi$ and so with v given by (3.9) we can integrate to have

$$u = \int_{\pi/4}^{\phi} U \sin\phi'\,d\phi' = U(2^{-1/2} - \cos\phi). \tag{3.10}$$

We conclude that the flow across the slip-lines increases from zero across the rigid/plastic flow boundary OC to a value on the interface which is a function of the wedge angle Ω subtended by the soil surface within a radial distance of OC from the barrier top as shown in Figure 6. The total flux across OD must balance that across CD to ensure that all the soil entering the plastic zone is expelled over the top of the barrier, as required for steady state. As deduced earlier, the pressure is constant along the individual rays, and the α slip-line result (3.8a) means that the pressure increases from the atmospheric value (taken as zero) along OD to a maximum value of $p(\pi/4) = 2k\Omega$. The horizontal stress acting on the rigid dead soil surface interface OC is transmitted through to the barrier OS, so that the net horizontal force acting on the barrier due to the soil is given by

$$-\sigma_x S = (p(\pi/4) + k)S = (2k\Omega + k)hl,$$

where $S = hl$ is the surface area of the barrier making contact with the soil. Additional to this dynamic pressure, there is a hydraulic pressure $(\rho gh/2)S$ that needs to be overcome, so that the overall force applied by the soil on the barrier is

$$F_s = -\sigma_x S + (\rho_s gh/2)S = (2k\Omega + k + \rho_s gh/2)hl. \tag{3.11}$$

We need also make mention of soil in the region above the slip-line OD in Figure 6. Any such material is outside the range of influence of the barrier and so will not be affected by it, although as it has been expelled from the plastic zone OCD it moves with speed $u(\pi/4 + \Omega)$, where $u(\phi)$ satisfies equation (3.10). Evidently this will be projected over the barrier and will pile up on or around the truck. The trajectories of the rocks could be calculated using simple dynamics, but since these particles cannot affect the force acting on the barrier, there is no need to do this. Of more importance is the wedge angle Ω. The line OD which determines the wedge angle Ω is tangential to the soil surface within the range given by the ray OC, and this angle will grow as the barrier penetrates further into the soil pile. Initially we might expect that $\Omega = \pi/4$, which eventually becomes $3\pi/4$ when the barrier becomes fully engulfed in the bund.

Our soil analysis has several important implications for the practical design of a suitable barrier. We reiterate that it is only the soil that lies within the plastic flow wedge-shaped zone that plays a role in determining the soil force associated with yielding. In consequence, the resistance force is governed only by the barrier geometry, particularly its height and, perhaps surprisingly, is independent of the speed of the truck. This means that our previous very simple argument leading to the prediction of the penetration distance x_p given by (2.1) and based on the assumption that the resistive force does not depend on U might be more useful than anticipated. Our calculations also suggest that there is little to be gained by constructing a very large pile of soil behind the barrier except perhaps immediately over its footing. Any excess bund further away from the barrier fulfils no purpose in contributing to the force applied by the bund. Lastly, we comment again that it is the soil resistance due to yielding that dominates the situation, and the contribution arising from the friction with the ground is relatively small.

4. Field experiments

In order to benchmark the effectiveness of the proposed barrier design, a series of tests were carried out in August 2016 at the Edna May gold mine waste dump in Westonia, Western Australia about 300 km east of Perth. Twenty four individual polyethylene units were lined up on a flat area, and a CAT 992 loader carefully placed rock material from the gold mine behind the EP units. This operation is shown in Figure 3. A series of experiments were conducted using two distinct material types (a fresh rock and an oxide rock) and three bund heights of 2 m, 2.5 m and 3 m. Force was applied to a pair of adjacent units using a load test frame and a dozer. The test frame is shown in Figure 7, and its size was chosen to be comparable to that of the width of a small dump truck. The minimum force needed to completely move the bund so that it did not revert to its original position was measured. The dozer was unable to deliver sufficient force to mobilize the largest 3 m high bunds for, when forces of 600 kN were reached, the dozer began to lose traction. Some minor local damage was observed on a few of the EP units but in the main the units remained vertical, intact and connected, and thus effectively transmitted the applied force through to the bund. The experimental aspect of the project is not the focus of this paper, and fuller details of the field set-up may be found in [4].

The observed behaviour of the performance of the barrier was consistent with the theoretical predictions made earlier. The moving barrier was seen to transport a wedge of rock and soil, while the displaced soil outside this wedge moved up and over the top. Recall that the net effect is to produce a resistance to the barrier movement made up of two components; a soil resistance acting at right angles to the barrier and frictional resistances acting underneath the barrier itself but, arguably more importantly, under the wedge of soil and rock moving with the barrier. Our simple model of this situation predicts the total barrier resistance force to be given by (2.3), where the shear strength of the rock material at Edna May is about $S_{\max} = 200\ \mathrm{kNm}^{-2}$. With our expectation that the resistance force is essentially independent of truck speed U and acts instantaneously, the penetration distance x_p due to the impact has already been shown to be given by equation (2.1). Shown in Figure 8 are some sample measurements relating to the two soil types used. The experimental results are only weakly dependent on the type of soil used and match up well with

FIGURE 7. A load test frame as applied to the EP units during a physical testing at the Edna May gold mine.

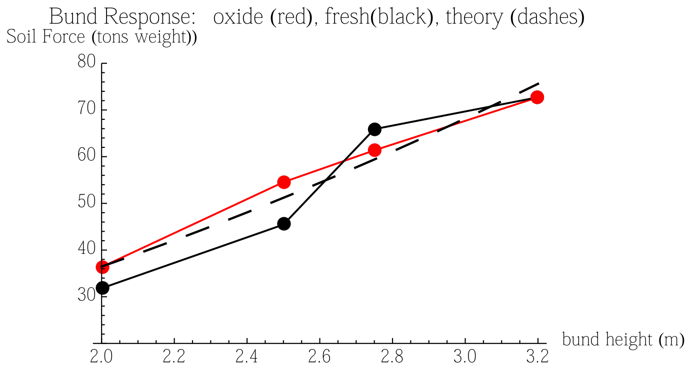

FIGURE 8. A simple comparison of field data obtained at the Edna May site compared to the theory developed in this paper. The two solid lines show the soil force resistance as a function of the bund height for the two soil types. Shown dashed line is the theoretical prediction of this dependence according to the result (3.11).

the theory. These preliminary findings give confidence that the underlying physics used to derive our predictions is appropriate, and sets the scene for more extensive and comprehensive experiments that will be reported elsewhere.

4.1. Oblique truck/barrier incidence In practice, of course, it is unlikely that a truck will strike the barrier head-on, and it is more probable that the impact will be of a more glancing nature. In this scenario, the two-dimensional nature of the head-on motion becomes truly three dimensional, and then the complicated interaction geometry makes it impossible to predict the subsequent behaviour. This would require a full-scale numerical simulation, but some qualitative remarks can be made. It is

https://doi.org/10.1017/S1446181117000281 Published online by Cambridge University Press

expected that if the truck hits the barrier at an angle θ to the barrier then the normal component of velocity is given initially by $U \sin\theta$, and this will be reduced to zero by the barrier resistance F_b over a time $t_0 = U \sin\theta / F_b$. Simultaneously, the truck will slide along the barrier with the tangential velocity that is reduced due to contact friction of magnitude μF_b, where μ is the effective sliding coefficient of friction between the vehicle and the barrier. After the normal velocities of the barrier and truck reduce to zero, there may be a small elastic rebound due to the energy stored in the barrier filler. One issue that requires careful consideration is the effective size of the sliding coefficient μ, and this is likely to be critically dependent on the part of the truck that hits the wall. If the contact is primarily with the tyres, the coefficient of friction between rubber and other materials can be large (and can even exceed unity on occasions). Then the truck may stick to, or penetrate, the barrier in which case it may rotate to face the barrier owing to the torque acting. More often, one might expect the truck to slide down the barrier with several individual units.

Some further experiments were performed for oblique contact. A typical dump truck is nearly 8 m wide so that four linked panels can resist its motion. Measurements suggested that an empty 200 tonne truck moving at 20 km hr^{-1} normal to a 2 m high bund would push the barrier back about 4.2 m. If the truck made a glancing impact at an angle of about 20 degrees, the corresponding penetration distance was much smaller; about 0.5 m. If the bund was higher and raised to 3.2 m, the corresponding results were 3 and 0.34 m, respectively. For a fully loaded truck weighing about 500 tonnes and travelling at 10 km hr^{-1}, a bund height of 3.2 m would be sufficient to reduce the normal impact penetration distance to about 0.15 m. Of course, in the absence of a three-dimensional generalization of our theory, it is not easy to predict the likely penetration distance in the eventuality of an oblique incidence. Fortunately, we can be reasonably sure that the normal incidence problem represents in some sense the worst-case scenario, so at least those findings can be used as a very conservative guide as to the likely behaviour, should the truck strike the barrier at an oblique angle.

5. Concluding remarks

In this work, we have developed a simple theory to predict the stopping distance of a truck when it impacts a vertical barrier behind which lies a supporting bund. While the mathematics for describing the dynamics of the truck is almost trivial, the description of the motion of the soil is less easy. An exact solution of the relevant plastic flow equations suggests that the main component of the resistive force acting on the truck arises from the soil. Our predictions have been backed up by some fieldwork, the results of which suggest that the analysis of behaviour of the proposed barrier system is consistent with what is seen in practice.

The barrier by itself provides little resistance to the moving truck, but needs to push against the bund to activate the soil force; in effect, the barrier simply acts as an agent for transmitting this large soil heaving force to the moving dump truck. Most importantly, from both experimental and theoretical perspectives, the resistance force to bund movement seems to be velocity independent. The critical shear stress required to set the soil in motion will depend not only on the soil type and its composition (through $S_{\max}$) but also on the soil depth; it is the hydrostatic component of the stress that dominates. Thus, it is the combination of the weight and height of the bund immediately behind the barrier that primarily determines its effectiveness. Thus, accurately tuning the barrier design to deal with different soil/rock types would appear to be not normally necessary.

It should be noted that the resistance force is speed independent, and increases rather rapidly with the barrier and soil pile height. The upshot is that fine-tuning adjustments required to deal with any one specific mining situation need not be particularly dramatic; normally a change in bund (rather than the barrier) height would be required. The presence of the barrier will prevent the truck from climbing up on the bund, unless the barrier totally collapses under impact, so needs to remain substantially intact under the impact. The experiments show that the barrier does hold back the soil and does not break up under the imposed forces of the experiment. The strut behind the barrier serves to inhibit buckling along a horizontal axis, and the protruding base of the barrier plays the same role along a vertical axis. Evidently, an oblique truck impact could increase the buckling torque while an increase in buckling strength could be achieved by using a supporting cable passing along the barriers, but this may prove not to be necessary.

To finish, we comment that this work shows how elementary and long-established mathematics can be used to tackle real problems thrown up by industry. Our findings here have provided a benchmark for a more extensive suite of experiments, and played a small part in the design of a product that is now available on the market [8].

Acknowledgement

The referees are thanked for a number of comments that helped improve the clarity of the paper.

References

[1] P. L. Capper and W. F. Cassie, *The mechanics of engineering soils*, 6th edn (John Wiley, New York, 1976).

[2] P. C. Chan, "Shear strength of soils subjected to a single rapid loading", in: *Proc. 5th engineering mechanics division speciality conf., Wyoming,* Volume 2 (ASCE, New York, 1984) 1328–1331.

[3] K. T. Chau, *Analytic methods in geomechanics* (CRC Press, Boca Raton, FL, 2013).

[4] S. Durkin, N. Fowkes, N. Redwood and A. P. Bassom, "Innovative approach to open pit edge protection", in: *Proc. ninth AusIMM open pit operators' conf., Kalgoorlie, WA* (AusIMM, Melbourne, VIC, 2016) 138–149.

[5] R. Hill, *The mathematical theory of plasticity*, *Oxford Engineering Science Series* (Clarendon Press, Oxford, 1950).

[6] P. G. Joseph, "A dynamical systems-based approach to soil shear", *Géotechnique* **60** (2010) 807–812; doi:10.1680/geot.9.P.001.

[7] J. Lubliner, *Plasticity theory* (Dover, New York, 2008).

[8] Safescape, http://www.safescape.com/edge-protector-ep/.